REFERENCES AND NOTES

1. P. R. Watson, M. A. Van Hove, K. Herrmann, Eds., *Atlas of Surface Structures* (*J. Phys. Chem*. Ref. Data, Monogr. No. 5, American Institute of Physics, New York, 1995).
2. D. Menzel, *Surf. Rev. Lett.* **4**, 1283 (1997).
3. R. E. Martinez, W. A. Augustyniak, J. A. Golovchenko, *Phys. Rev. Lett*. **64**, 1035 (1990); A. J. Schell-Sorokin and R. M.Tromp, *ibid.*, p. 1039.
4. V. Buck, *Z. Phys. B* **33**, 349 (1979); D. Sander and H. Ibach, *Phys. Rev. B* **43**, 4263 (1991).
5. R. Schuster, H. Röder, K. Bromann, H. Brune, K. Kern, *Phys. Rev. B* **54**, 13476 (1996); G. Ritz, M. Schmid, A. Biedermann, P. Varga, *ibid.* **53**, 16019 (1996).
6. E. Kampshoff, E. Hahn, K. Kern, *Phys. Rev. Lett.* **73**, 704 (1994).
7. H. Trinkaus, *Radiat. Eff.* **78**, 189 (1983).
8. M. Schmid, W. Hebenstreit, P. Varga, *Phys. Rev. Lett.* **76**, 2298 (1996).
9. H. Ullmayer, *Radiat. Eff.* **78**, 1 (1983).
10. M. Lindroos, H. Pfnür, G. Held, D. Menzel, *Surf. Sci.* **222**, 451 (1989).
11. H. Pfnür, G. Held, M. Lindroos, D. Menzel, *ibid.* **220**, 43 (1989).
12. No Fourier or other filtering was applied, but the contrast was adjusted to make the structures in the very different regions visible simultaneously.
13. At low-oxygen coverages $\Theta_O < 0.1$ ML, oxygen atoms have high mobility at room temperature, and their average residence time per lattice site (0.05 s) is smaller than that required for their complete imaging. However, because of the line-by-line scanning of the STM image, fast-moving oxygen atoms can be easily recognized by the horizontal dashes that correspond to incomplete images of them.
14. M. Gsell, P. Jakob, D. Menzel, data not shown.
15. K. L. Kostov *et al.*, *Surf. Sci. Lett.* **394**, L138 (1997).
16. G. Michalk, W. Moritz, H. Pfnür, D. Menzel, *Surf. Sci.* **129**, 92 (1983).
17. D. Menzel, *ibid.* **318**, 437 (1994), and references given therein.
18. M. Mavrikakis, B. Hammer, J. K. Nørskov, private communication.

19. Supported by the Deutsche Forschungsgemeinschaft through Sonderforschungsbereich 338.

7 January 1998; accepted 10 March 1998

Micromechanical "Trampoline" Magnetometers for Use in Large Pulsed Magnetic Fields

V. Aksyuk,* F. F. Balakirev, G. S. Boebinger, P. L. Gammel, R. C. Haddon,† D. J. Bishop

A silicon micromechanical magnetometer was constructed and successfully used in 60-tesla pulsed magnetic fields of less than 100-millisecond duration. The device is small, inexpensive to fabricate, and easy to use. It features a fast mechanical response (up to 50,000 hertz) and extremely high sensitivity yet is relatively robust against electrical and mechanical noise. Quantum oscillations in the magnetization of a 1-microgram sample of an organic superconductor, κ-[bis(ethylenedithio)tetrathiafulvalene]$_2$Cu(NCS)$_2$, have been observed with this device.

Pulsed magnetic fields exceeding 30 T have recently become more readily available to small laboratory-based research groups. The discharge of a large bank of capacitors through a compact solenoid composed of several hundred turns of wire with a very high tensile strength generates a rapid high-field magnetic pulse. The pulse duration (typically a few tens of milliseconds) and repetition rate (three pulses per hour) are both limited by the substantial heating of the solenoid during the pulse.

Making accurate measurements in pulsed magnets can be a challenge because of the short duration of the pulses and the considerable electrical and acoustical noise in the sample environment. Furthermore, although magnets of this design can survive as many as 1400 60-T pulses, stress on the solenoid may on occasion lead to explosive failure during a pulse. Thus, experimental probes need to be reasonably reproducible and relatively inexpensive.

We report here on a micromachined silicon "trampoline" device that allows magnetization to be measured for a wide range of solids with high sensitivities over time scales consistent with the decay times of a typical pulsed magnet. The magnetometer operates as a Faraday balance: When placed in a magnetic field gradient, a sample experiences a force proportional to the magnetization of the sample multiplied by the magnitude of the field gradient. If the sample is attached to a spring, measuring the sample displacement is equivalent to measuring the force exerted by the magnetic field gradient. A scanning electron microscope image (Fig. 1A) of the magnetometer shows the square micromachined polysilicon plate, typically 300 to 500 μm on a side, that is freely suspended by four soft springs, one at each corner. One of the four springs is shown in Fig. 1B. When mounted, the sample is affixed to the center of the polysilicon plate and both are free to move vertically together by an amount, δz, in response to the force, $\mathbf{F} = \nabla(\mathbf{M}\cdot\mathbf{B})$, where $\mathbf{M}$ is the magnetization of the sample and $\mathbf{B}$ is the magnetic field (*1*). In practice, this displacement is detected by measuring the capacitance (from 0.3 to 1.1 pF) between the mobile polysilicon plate and a fixed polysilicon plate of the same size (not visible in Fig. 1), located directly under the mobile plate.

The two plates are separated by a ~2-μm gap created by the etching of an SiO_2 sacrificial layer, a process that was facilitated by an array of small etch holes 20 μm apart in the mobile plate (Fig. 1B). An array of small posts (60 μm apart) protrudes from the bottom of the mobile plate to prevent the two plates from touching and adhering to one another. The capacitance measurement can be made on a very short time scale (~30 μs), with a resolution as high as 1 part in 10^4, by the application of a 1-V, 100-kHz excitation to the leads. For the device to have a high sensitivity to the magnetization of the sample, the springs must be soft enough (~1 N m^{-1}) to allow a measurable displacement in response to very small forces. Silicon surface micromachining allows a wide latitude in designing the mechanical properties of the magnetometer plates and springs without reducing the mechanical robustness of the suspended polysilicon plate (*2*).

The magnetometer is best suited to small samples, which tend to be more homogeneous than large samples and more immune to unwanted heating (which can result from eddy currents induced in the sample by the pulsed magnetic field). Its small size results in high mechanical resonant frequencies (typically >10 kHz, which can be tuned by altering the design of the springs), which yields sufficiently fast mechanical response times. Although the pulsed magnet generates mechanical vibrations during the pulse, this mechanical noise occurs at much lower frequencies (<100 Hz) and thus couples very little to the mechanical resonances of the magnetometer.

We confirmed the desired operation of the magnetometer by measuring the mechanical response of the structure to applied electric fields. To determine the mechanical resonance frequencies of the magnetometer, we measured the displacement between the magnetometer plates with a lock-in amplifier while the frequency of a 1-mV ac excitation voltage was swept from nearly dc up through the various resonant frequencies of the device. The lowest resonant frequency, f_{res}, of the particular device used in the experiments described below to de-

V. Aksyuk, P. L. Gammel, R. C. Haddon, D. J. Bishop, Bell Laboratories, Lucent Technologies, Murray Hill, NJ 07974, USA.
F. F. Balakirev and G. S. Boebinger, Bell Laboratories, Lucent Technologies, Murray Hill, NJ 07974, USA, and Los Alamos National Laboratory, MS E536, Los Alamos, NM 87545, USA.

*To whom correspondence should be addressed. E-mail: aksyuk@physics.bell-labs.com
†Present address: Departments of Chemistry and Physics, University of Kentucky, Lexington, KY 40506, USA.

tect quantum oscillations was measured to be 9.85 kHz, which implies a spring constant k of 1.2 N m^{-1} (*3*). We determined the displacement of the mobile plate in response to an applied dc electric field (circles in Fig. 1C) by measuring the change in capacitance of the magnetometer with field. Near $V^2 = 8.6$ V^2, the mobile plate discontinuously jumps toward the fixed plate and comes to rest on the offset posts (which are 0.75 μm tall). This instability is intrinsic to parallel plate capacitors (the solid line in Fig. 1C indicates the expected behavior for an ideal parallel plate capacitor). Excellent agreement with the data was obtained, even with the spring constant, $k = 1.2$ N m^{-1}, constrained to the value determined from the ac measurements. These measurements leave only two free fit parameters: the zero-bias spacing (2.72 μm) and the inclusion of a fixed, parallel stray capacitance (0.02 pF, a reasonable value for the stray capacitance between the leads to the magnetometer).

To test our magnetometer design for pulsed magnetic field applications, we mounted a 0.8-μg sample of the superconducting (transition temperature ~10 K) organic compound κ-(BEDT-TTF)$_2$Cu(NCS)$_2$ [where BEDT-TTF is bis(ethylenedithio)tetrathiafulvalene] on the magnetometer, oriented so that the magnetic field could be applied perpendicular to the conducting planes (*4*). This compound displays quantum oscillations that arise from the two-dimensional Fermi surface of this material. Such oscillations are periodic as a function of inverse magnetic field and occur in clean metals when the quantized orbits of the electrons in the field coincide with the orbits at the Fermi surface. Quantum oscillations in resistivity have been seen in κ-(BEDT-TTF)$_2$Cu(NCS)$_2$ with the use of both dc (*5*) and 50-T pulsed magnetic fields (*6*). To date, quantum oscillations in magnetization have been observed in dc magnetic fields (*7*) but not in pulsed magnetic fields.

The sample and magnetometer were placed in superfluid liquid He at 1.7 K and positioned 1 cm above the magnetic field center, where the peak magnetic field and gradient were 60.0 T and 1.4 T cm^{-1}, respectively (Fig. 2, A and B). Because of the short length (~10 cm) of the solenoid we used (*8*), the magnetic field developed extremely large gradients (as high as 18 T cm^{-1}) away from the center of the magnet. During the pulse, whose time profile is shown in Fig. 2A, an oscillating magnetization in the sample produced a time-varying force. The resulting displacement was detected capacitively with a standard bridge circuit (*9*). The quantum oscillations of the magnetization of the organic superconductor κ-(BEDT-TTF)$_2$Cu(NCS)$_2$ were clearly seen during the 60-ms downsweep of the magnetic field (Fig. 3A). Because of the designed spring stiffness of this particular magnetometer, the quantum oscillations were not observed during the 6-ms upsweep

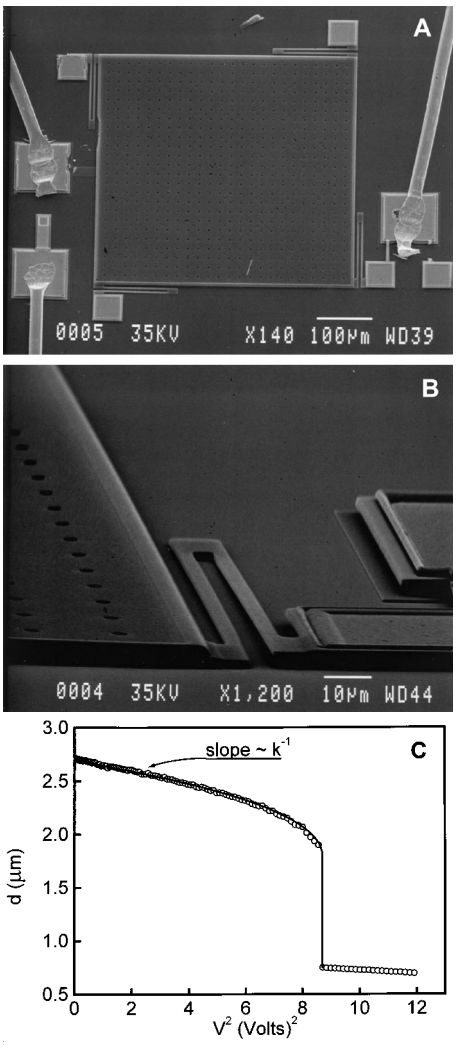

Fig. 1. Scanning electron micrographs of (**A**) an example of the Si micromachined magnetometer and (**B**) a close-up of one of the four springs on the polysilicon plate. Electrical connection to the fixed capacitor plate is made through the wire-bonded lead seen on the upper left of (A). Electrical connection to the mobile plate is made through the wire-bonded lead shown on the right in (A), where the polysilicon spring itself provides the electrical connection to the mobile plate. The polysilicon used to build the plate typically gives a sheet resistivity of 20 ohms per square for the plate. (**C**) The displacement of the plate as a function of an applied dc voltage. The data are the open circles, and the theory described in the text is represented by the solid line.

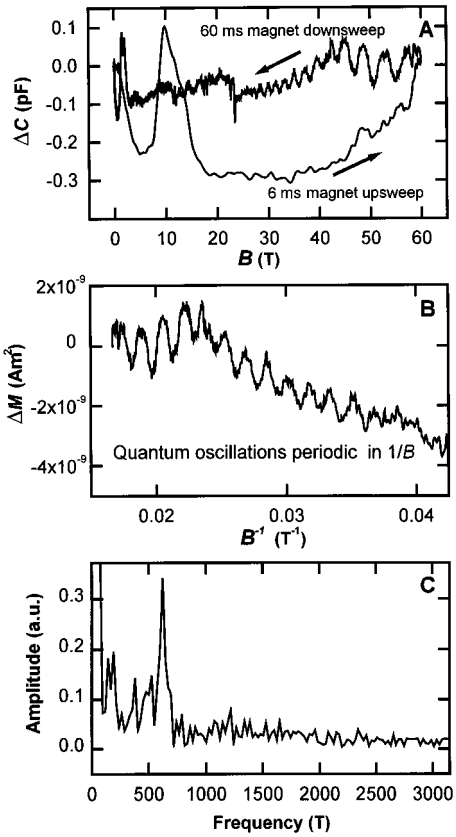

Fig. 3. Data taken on the organic superconductor κ-(BEDT-TTF)$_2$Cu(NCS)$_2$ using the Si micromachined magnetometer and the pulsed field magnet. (**A**) The raw capacitance data versus the applied field **B**. (**B**) The sample magnetization Δ**M** versus **B**$^{-1}$. (**C**) The Fourier transform of the magnetization. These data verify that the quantum oscillations are periodic in **B**$^{-1}$ and have the correct frequency for the compound studied.

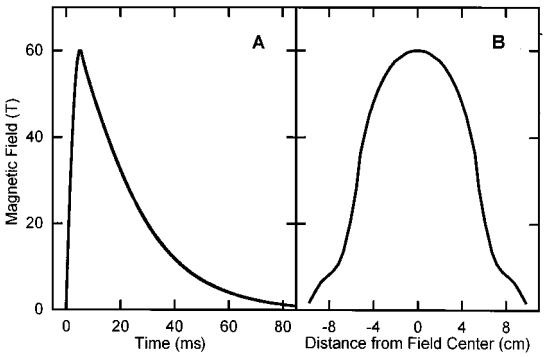

Fig. 2. (**A**) The time profile of the magnet pulse. (**B**) The field profile of the pulsed magnet (*8*).

of the magnetic field because they occur too quickly. This particular magnetometer has its resonant frequency at $f_{res} \sim 10$ kHz when unloaded, which decreases to an estimated value of 5 kHz when loaded with the ~0.8-μg sample. Shown in Fig. 3B is the calibrated magnetization of the sample versus inverse magnetic field. The quantum oscillations are periodic in the inverse magnetic field with a frequency of 615 ± 20 T, in good agreement with the accepted value of 600 ± 5 T (*5*–*7*) (Fig. 3C).

The data we report were taken on a sample roughly two orders of magnitude smaller in mass than is typical for magnetization measurements (*7*, *10*, *11*). Pulsed-field magnetization studies of two-dimensional organic compounds have long been accomplished with magnetometers composed of compensated counterwound coils (*10*). The "trampoline" magnetometer and the counterwound coil magnetometer complement each other because the latter is particularly well suited for large samples and samples with rapid quantum oscillations. An alternate Si micromachined magnetometer design, the cantilever magnetometer (*11*), competes more directly with the trampoline magnetometer. This type of magnetometer uses a micromachined Si cantilever beam that holds the sample. The reported noise values are comparable to those for our trampoline magnetometer, although to date the cantilever magnetometer design is limited to a frequency response below 1 kHz and therefore has been demonstrated only up to peak magnetic fields of 36 T in longer pulse magnets (~1-s duration).

The observed root-mean-square noise level of 7×10^{-11} A m^2 was measured with only a 30-μs time constant and corresponds to a noise figure of $\sim 10^{-12}$ A m^2 Hz$^{-1/2}$. This measurement was not limited by the noise generated during the pulsed magnetic field, even though no special effort was taken to isolate the magnetometer from vibrations induced by the pulsed magnet. Thus, there is substantial room for improvement. We recently achieved a tenfold improvement in the resolution of capacitance measurements during the 60-T pulsed magnetic field, which reduces the measured noise figure to $\sim 10^{-13}$ A m^2 Hz$^{-1/2}$. We have also tested newer magnetometer designs, with springs 25 times as stiff (f_{res} up to 50 kHz), with the goal of accessing still higher frequency quantum oscillations.

REFERENCES AND NOTES

1. There are two relevant limits: (i) the "hard spring limit," in which our device operates, where $\mathbf{F} = k\,\delta\mathbf{z}$ (k is the total spring constant), and (ii) the "soft spring limit," in which $\mathbf{F} = md^2\mathbf{z}/dt^2$ (m is the total mass of the mobile plate plus sample).
2. For example, the magnetometer can survive being dropped on the floor, although we do this as infrequently as possible.
3. Given the 300 μm by 300 μm by 1.5 μm size of that mobile plate, its mass can be calculated to be 0.31 μg, from which k was determined to be 1.2 N m^{-1}. No significant change in f_{res} or k was observed between room temperature and 4.2 K.
4. The growth and characterization of the samples are described in R. C. Haddon, S. H. Glarum, S. V. Chichester, A. P. Ramirez, N. M. Zimmerman, *Phys. Rev. B* **43**, 2642 (1991).
5. J. Caulfield *et al.*, *J. Phys. Condens. Matter* **6**, 2911 (1994).
6. N. Harrison *et al.*, *ibid.* **8**, 5415 (1996).
7. F. A. Meyer *et al.*, *Europhys. Lett.* **32**, 681 (1995).
8. G. S. Boebinger, A. Passner, J. Bevk, *Physica B* **201**, 560 (1994).
9. We tuned the bridge current to zero before the pulse by matching an external capacitance to the capacitance of the magnetometer. During the pulse, we detected the bridge output current using the built-in current-sensing preamplifier of a Stanford Research SR850 lock-in amplifier, whose fast output was fed into a 12-bit Hewlett-Packard HP5183 transient digitizer.
10. N. Harrison *et al.*, *Phys. Rev. B* **52**, 5584 (1995).
11. M. J. Naughton *et al.*, *Rev. Sci. Instrum.* **68**, 4061 (1997).

12. The work of F.F.B. is supported by the U.S. Department of Energy through Los Alamos National Laboratory.

8 December 1997; accepted 13 March 1998

Reductive Dechlorination of DDE to DDMU in Marine Sediment Microcosms

John F. Quensen III,* Sherry A. Mueller, Mahendra K. Jain, James M. Tiedje

DDT is reductively dechlorinated to DDD and dehydrochlorinated to DDE; it has been thought that DDE is not degraded further in the environment. Laboratory experiments with DDE-containing marine sediments showed that DDE is dechlorinated to DDMU in both methanogenic and sulfidogenic microcosms and that DDD is dehydrochlorinated to DDMU three orders of magnitude more slowly. Thus, DDD does not appear to be an important precursor of the DDMU found in these sediments. These results imply that remediation decisions and risk assessments based on the recalcitrance of DDE in marine and estuarine sediments should be reevaluated.

DDT [1,1,1-trichloro-2,2,bis(*p*-chlorophenyl)ethane] was one of the first synthetic pesticides to gain wide acceptance. Initially its use greatly enhanced crop yields, but pest species rapidly developed resistance so that its use in agriculture in the United States began to decline by 1959. It was effective longer in controlling mosquito-borne malaria (*1*) and is still used for that purpose in some tropical countries.

Because of environmental concerns, the use of DDT was banned in the United States and in some other countries in the early 1970s. By that time, however, it was distributed globally. Both DDD [1,1-dichloro-2,2,-bis(*p*-chlorophenyl)ethane] and DDE [1,1-dichloro-2,2,-bis(*p*-chlorophenyl)-ethylene] existed as by-products in commercial DDT formulations, and both may be formed by environmental degradation of DDT. DDT, DDD, and DDE (collectively DDX) are found, in various proportions, in soils and sediments and have been reported at 3422 out of 22,000 sites identified as posing a danger to humans and animal life by the U.S. Environmental Protection Agency (EPA) in its National Sediment Quality Survey.

One such marine site is the continental shelf off of the Palos Verdes Peninsula in southern California. Sediment core data collected over the last two decades by the Los Angeles County Sanitation District and the U.S. Geological Survey show that DDE is the most prevalent of the DDX compounds present in the shelf sediments and imply that the mass of DDE is decreasing with time (*2*, *3*). Bioturbation has been proposed as a mechanism responsible for this trend (*3*) because DDE is viewed as a recalcitrant compound (*4*). However, the concentration of trace metals in the sediments has remained constant with time, which is not consistent with bioturbation (*5*), and there is precedence for believing that DDE can be reductively dechlorinated to DDMU (*6*), which is also found in the sediment (*2*, *3*). Thus, an alternative explanation for the disappearance of DDE from the sediments, first proposed by List (*7*), is that it is being reductively dechlorinated to DDMU by

J. F. Quensen III, MBI International, 3900 Collins Road, Post Office Box 27609, Lansing, MI 48909–0609, and Center for Microbial Ecology, Michigan State University, East Lansing, MI 48824, USA.
S. A. Mueller and M. K. Jain, MBI International, 3900 Collins Road, Post Office Box 27609, Lansing, MI 48909–0609, USA.
J. M. Tiedje, Center for Microbial Ecology, Michigan State University, East Lansing, MI 48824, USA.

*To whom correspondence should be addressed. E-mail: quensenj@pilot.msu.edu